Title

Radiogenomics and Imaging Phenotypes in Glioblastoma: Novel Observations and Correlation with Molecular Characteristics

Journal

Current Neurology and Neuroscience Reports, 15(1)

ISSN

1528-4042

Author

Ellingson, BM

Publication Date

2015

DOI

10.1007/s11910-014-0506-0

Peer reviewed

Curr Neurol Neurosci Rep (2015) 15:506
DOI 10.1007/s11910-014-0506-0

NEURO-ONCOLOGY (LE ABREY, SECTION EDITOR)

Radiogenomics and Imaging Phenotypes in Glioblastoma: Novel Observations and Correlation with Molecular Characteristics

Benjamin M. Ellingson

Published online: 20 November 2014

Abstract Radiogenomics is a provocative new area of research based on decades of previous work examining the association between radiological and histological features. Many generalized associations have been established linking anatomical imaging traits with underlying histopathology, including associations between contrast-enhancing tumor and vascular and tumor cell proliferation, hypointensity on pre-contrast T1-weighted images and necrotic tissue, and associations between hyperintensity on T2-weighted images and edema or nonenhancing tumor. Additionally, tumor location, tumor size, composition, and descriptive features tend to show significant associations with molecular and genomic factors, likely related to the cell of origin and growth characteristics. Additionally, physiologic MRI techniques also show interesting correlations with underlying histology and genomic programs, including associations with gene expression signatures and histological subtypes. Future studies extending beyond simple radiology–histology associations are warranted in order to establish radiogenomic analyses as tools for prospectively identifying patient subtypes that may benefit from specific therapies.

Keywords Radiogenomics · Imaging genomics · GBM · Imaging phenotypes

This article is part of the Topical Collection on *Neuro-Oncology*

B. M. Ellingson
UCLA Brain Tumor Imaging Laboratory (BTIL), Center for Computer Vision and Imaging Biomarkers (CVIB), David Geffen School of Medicine, University of California—Los Angeles, Los Angeles, CA, USA

B. M. Ellingson
UCLA Neuro-Oncology Program, David Geffen School of Medicine, University of California—Los Angeles, Los Angeles, CA, USA

B. M. Ellingson
UCLA Brain Research Institute (BRI), David Geffen School of Medicine, University of California—Los Angeles, Los Angeles, CA, USA

B. M. Ellingson (✉)
Department of Radiological Sciences, David Geffen School of Medicine, University of California—Los Angeles, 924 Westwood Blvd, Suite 615, Los Angeles, CA 90024, USA
e-mail: bellingson@mednet.ucla.edu

B. M. Ellingson
Department of Biomedical Physics, David Geffen School of Medicine, University of California—Los Angeles, Los Angeles, CA, USA

B. M. Ellingson
Department of Bioengineering, Henry Samueli School of Engineering and Applied Science, University of California—Los Angeles, Los Angeles, CA, USA

Introduction

Brain tumors are considered a relatively rare cancer, affecting nearly 21 per 100,000 people in the USA [1]. Despite this relatively low incidence and the application of very aggressive combination therapies, malignant brain tumors are almost uniformly lethal. Glioblastoma multiforme (GBM) is the most common, aggressive, and fatal type of malignant glioma, accounting for 45 % of all malignant primary brain and CNS tumors and carrying a median survival of around 14 months [2] with fewer than 10 % of patients surviving beyond 5 years from initial diagnosis [3]. This dismal prognosis is largely attributed to molecular and genomic heterogeneity [4•], leading to variable treatment responses, as well as infiltrative tumor cells otherwise undetected with current imaging technology. Thus, great effort has been taken to advance the technology in the fields of molecular biology, genetics, and

radiology in order to better characterize individual patient tumor biology and behavior.

The progression of pathological and radiological sciences has largely been advancing in parallel over the decades, with very little formal cross-pollination until relatively recently. Molecular and genomic characterization of GBM has uncovered distinct phenotypes that appear to have differential prognosis and response to therapy. For example, GBM tumors exhibiting hypermethylation of the O^6-methylguanine-DNA-methyltransferase (MGMT) gene have been shown to have improved prognosis due to increased sensitivity to alkylating agents such as temozolomide, carmustine (BCNU), and lomustine (CCNU) [5, 6, 7•]. Additionally, both Verhaak et al. [4•] and Phillips et al. [8•] identified distinct molecular subclasses of high-grade gliomas with significantly different prognoses. Concurrent with these observations, radiologists and imaging scientists have uncovered a variety of radiographic features that provide insight into aggressivity and biology of malignant gliomas. For example, GBM typically contains central areas of necrosis, thickened irregular walls that enhance after administration of exogenous contrast agents, and is surrounded by regions of relatively extensive vasogenic edema. Many investigators have noted that the extent of these features, namely necrosis and the amount of edema, is associated with differences in survival [9–11, 12•, 13••]. Radiogenomics (or imaging genomics), the study of the association between radiographic and pathologic features, represents a new horizon in cancer research that focuses on the intersection of these two diagnostic disciplines. The field of radiogenomics holds great promise of the eventuality of inexpensive, noninvasive phenotyping of tumors for use in individualized patient therapies or treatment strategies by inferring genomic or pathologic characteristics from radiographic information. The current manuscript summarizes the current status of radiogenomics and imaging-based phenotyping in GBM, and then integrates this information to provide predictions and future directions for the field.

Anatomical Imaging Pathology Associations

As the name implies, GBMs are known for their heterogeneity, which extends across multiple scales. In particular, GBMs are heterogeneous in their genetic and epigenetic makeup, levels of protein expression, metabolic or bioenergetic behavior, along with their microenvironment biochemistry and structural composition. The amalgamation of these various changes is manifested as abnormalities observed on both gross histology and radiographic images. This multiscale heterogeneity can vary both across patients as well as spatially throughout a single tumor, reflecting broad genetic alterations in the disease and local adaptations of the disease to microenvironmental cues, respectively. Indeed, early image-guided proteomic studies have shown that areas of nonenhancing tumor vary dramatically in their protein expression compared with that of contrast-enhancing tumor, suggesting a fundamental biological difference between these radiographically defined regions [14].

Despite this heterogeneity, there are many common characteristics of GBM recognized both radiographically and pathologically [15•]. For example, most GBMs (with certain exceptions discussed later) show enhancement after administration of exogenous contrast either on MRI or computed tomography (CT), which has been shown to be directly due to an increase in vascular permeability often accompanied by neovasculature as a consequence of malignancy [16, 17]. Careful biopsies of areas of contrast enhancement on CT have also been shown to contain the most proliferative areas of the tumor [18], as angiogenesis allows for tumor to proliferate at much higher rates [19]. In addition to enhancement on post-contrast anatomical images, most GBMs commonly exhibit the presence of necrosis, either centrally or diffuse, discernable as low attenuation on unenhanced CT or low signal intensity on pre-contrast T1-weighted MR images due to an increase in both intra- and extracellular mobile water. Additionally, all GBMs have regions of high T2-weighted MRI signal intensity, which reflects increased water mobility in areas of both edema and nonenhancing tumor. Differentiating edema and nonenhancing tumor can be difficult; however, numerous studies have shown that edema tends to be brighter on T2-weighted images compared to that with nonenhancing tumor [12•, 20••], which is directly due to edema having a longer tissue T2 and normal brain tissue having a shorter T2 compared with nonenhancing tumor [21–23]. Together, these attributes have formed the basis for biological justification in the use of CT and MRI as surrogates of tumor burden in GBM for use in therapeutic response assessment [24–27].

Anatomical MRI including T2-weighted images, T2-weighted fluid attenuated inversion recovery (FLAIR) images, along with pre- and post-contrast T1-weighted images are the modalities of choice for brain tumor imaging. MRI is typically chosen over other anatomical imaging techniques such as computed tomography (CT) due to the high contrast within soft tissues and high sensitivity for lesion delineation. Additionally, MRI is attractive because it does not involve ionizing radiation, and it is extremely flexible in that it can provide a variety of image contrasts based on quantum mechanical characteristics unique to the tissue (e.g., T1 and T2 characteristics), microscopic mobility of water molecules (e.g., T2 and diffusion MRI), oxygenation status (e.g., susceptibility and blood oxygenation level detection, or BOLD imaging), mobile metabolite concentration (e.g., MR spectroscopic imaging and chemical shift imaging), and other physiological parameters. Thus, the following radiogenomic discussion will focus almost exclusively on MRI features, as they are the most common encountered clinically.

Tumor Location May Reflect Cell of Origin

There is significant evidence to support the hypothesis that tumor location plays a pivotal role in patient prognosis [28]. This observation is likely reflective of genetic attributes of the tumor cells of origin [29, 30], as region-specific brain tumor cells of origin have been identified for oligodendrogliomas [31], medulloblastomas [32], ependymomas [33], and IDH1 mutant GBM [34]. Recently, we presented a widespread examination of the relationship between tumor location and various phenotypes and clinical variables in a "probabilistic radiographic atlas" of more than 500 GBM patients, noting several interesting and new associations [13••]. For example, younger patients (<55 years old) tend to have more frontal tumors, whereas older tumors tend to be localized more posterior; IDH1 mutant tumors tend to be localized to the frontal lobe and adjacent to cells near the subventricular zone (SVZ) [13••, 34]; and MGMT promoter methylated tumors tend to be more frequent in the left temporal lobe, whereas MGMT unmethylated tumors tend to be right hemispheric [13••, 35]. Interesting interactions were also noted, including a preference for MGMT unmethylated, mesenchymal, and epidermal growth factor receptor (EGFR)-amplified tumors to be localized to the right insula, thalamus, and temporal lobe regions extending to the posterior lateral ventricles adjacent to the SVZ (Fig. 1a, b), a region of the brain known to harbor adult stem cells. In fact, tumors growing in regions thought to contain neural stem cells have been shown to predict both invasive and multifocal radiographic phenotypes [36]. These regions were also associated with a high probability of having a short survival (overall survival (OS) <12 months) [13••]. In addition to these observations, there appears to be frontal predominance of younger, IDH1 mutant, chromosome 10 monosomy, and proneural tumors (Fig. 1c, d). Frontal lobe involvement and preference for the proneural subtype have previously been shown to be associated with IDH1 mutant GBMs [34, 37], as these types of tumors are hypothesized to develop from a specific cell of origin [34]. Separate regions in the left temporal pole extending to the left insula were also identified to be commonly associated MGMT methylated, EGFR-amplified, and EGFRvIII mutant GBMs. This region was also associated with a favorable response to radiochemotherapy (progression-free survival (PFS) >6 months) and favorable overall survival (OS >12 months) [13••]. Thus, it appears that radiographic atlases providing associations liking tumor location to various clinical, -omic, and interventional phenotypes may provide a valuable tool for potentially understanding the nature of brain tumor cells of origin and may be an intuitive starting point toward individualized medicine on the basis of radiogenomic phenotyping.

Associations Between Tumor Size and Molecular Characteristics

As alluded to previously, radiologic and pathologic attributes associated with poor prognosis were independently identified such that many broad generalizations of tumor biology can be deduced through the use of standard anatomical MRI. Relatively recently, investigators have begun to explore more complex associations between tumor size measurements and genetic or molecular composition. Our investigations [13••] at initial diagnosis have shown that MGMT unmethylated tumors tend to have higher volumes of both enhancement (T1 + C) and T2/FLAIR hyperintensity compared with methylated tumors (Fig. 2a), IDH1 mutant GBMs have a significantly lower volume of enhancement (Fig. 2b), and EGFR-amplified tumors have a significantly higher volume of both enhancement and T2/FLAIR hyperintensity (Fig. 2e). Interestingly, Diehn et al. [38] also noted that GBMs with overexpression of EGFR tended to have higher contrast-enhancing tumor volume. However, we have also noted no difference in enhancing or T2/FLAIR volumes in patients with chromosome 10 monosomy vs. polysomy (Fig. 2c), intact vs. deficient phosphatase and tensin homolog (PTEN) (Fig. 2d), or EGFRvIII mutants vs. wild types (Fig. 2f). Similarly, Naeini et al. [39•] demonstrated that volumes of both contrast enhancement and necrosis at the time of initial diagnosis are higher in tumors with the mesenchymal gene expression signature compared with those having proneural or proliferative signatures. This trend was also apparent when excluding IDH1 mutant tumors, which are known to be primarily in the nonmesenchymal molecular subtype. The authors noted that the volume of contrast enhancement plus necrosis could be used to identify the mesenchymal subtype with 76 % sensitivity and 65 % specificity, while the ratio of T2/FLAIR hyperintense volume to the volume of contrast enhancement plus necrosis less than 2.3 had an 82 % sensitivity and 87 % specificity of identifying the mesenchymal subtype.

Zinn et al. [40•] took a fundamentally different approach for examining the relationship between tumor volumetry and pathological features. Instead of examining volume differences between phenotypes with known prognostic or therapeutic phenotypes, investigators used data from The Cancer Genome Atlas (TCGA), quantified the volume of T2/FLAIR hyperintensity, binned the volumes into high, medium, and low volumes, and then examined which genes were upregulated or downregulated within these groups. Investigators identified an association between high T2/FLAIR volumes, upregulation of periostin (POSTN), and downregulation of miR-219, a microRNA predicted to bind with POSTN.

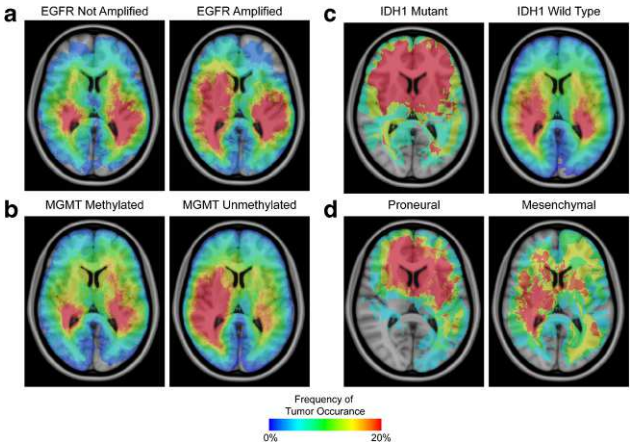

Fig. 1 Anatomical distribution of T2/FLAIR tumor locations for various genomic and molecular phenotypes. **a** EGFR-amplified tumors show a higher frequency of tumor location in the right hemisphere compared to that with tumors not exhibiting EGFR amplification. **b** Similarly, MGMT unmethylated tumors have a higher frequency of occurrence in the right hemisphere compared to that with methylated tumors. **c** GBMs with mutation of IDH1 show frontal lobe predominance compared to that with wild-type IDH1 tumors. **d** Correspondingly, the proneural gene expression subtype also appears to have frontal lobe predominance. Population maps were created from the University of California Cancer Research Coordinating Committee (UC CRCC)-sponsored probabilistic radiographic atlas [13••]

Investigators also noted high levels of POSTN found to be associated with mesenchymal tumors and shortened survival and further concluded that this approach may be valuable for identifying new targets for molecular inhibition or future therapies.

A separate study by Zinn et al. [41] also used data from the TCGA to develop a biomarker consisting of tumor volume–age–Karnofsky performance status (KPS) (VAK) to predict prognosis in GBM. Investigators determined the volume of contrast-enhancing tumor regions, and then categorized the volumes as being large or small using a 30-cm^3 cutoff threshold. The study found that patients with a favorable biomarker signature, consisting of either young patients, patients with a high KPS, or a small tumor volume, was associated with genomic and microRNA signatures consistent with programs involved in p53 activation, whereas an unfavorable biomarker signature was associated with programs involved in p53 inhibition.

In a TCGA study by Gutman et al. [42], investigators used semi-quantitative measurements of tumor size and radiographic composition. Trained radiologists from a range of institutions estimated total lesion size using bidirectional measurements on T2 or FLAIR images, then described the composition of the tumor by assigning percentages to the amount contrast-enhancing tumor, nonenhancing tumor, edema, and necrosis. These percentages were then binned by predefined ranges. Consistent with previous observations [13••, 37, 39•], investigators noted that proneural tumors had significantly lower proportions of contrast-enhancing tumor while mesenchymal tumors had lower levels of nonenhancing tumor.[1] Authors also examined whether there was a link between the radiographic composition of the tumor and mutation status (e.g., EGFR, IDH1, NF1, PIK3CA, PTEN, etc.) or copy number variations but did not find any significant associations.

Descriptive Radiographic Features and Genetic Composition

Although there appears to be associations between tumor location or tumor size and pathological markers, these simple measures fail to capture sophisticated features intuitively used by the neuroradiologist to diagnose and characterize the aggressivity and behavior of the tumor. Such descriptive radiographic features are difficult to quantify but are often invaluable in radiogenomic analyses in other cancers [43, 44]. Pope et al. [12•, 20••] first developed a set of semi-quantitative radiographic descriptive features for use in GBM in order to link these features with both survival and gene expression signatures. These investigators noted that tight junction protein-2 (zonula occluden-2), a protein that acts to maintain the BBB, was upregulated in incomplete enhancing tumor compared with contrast-enhancing tumor. Additionally, they noted that oligodendrocyte lineage transcription factor 2 (OLIG2) and achaete-scute complex-like 1 (ASCL1), which is associated with secondary GBM, were increased in

[1] Note: the previous work utilized the gene expression classification system by Phillips et al. [8•], whereas the work by Gutman et al. employed the classification system by Verhaak et al. [4•].

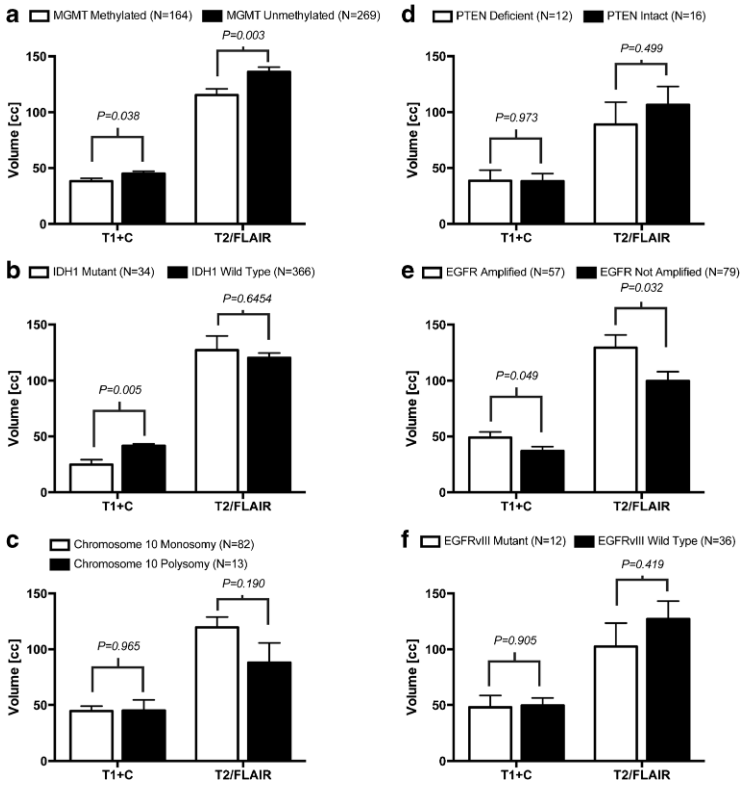

Fig. 2 Differences in tumor volume between various genomic and molecular phenotypes. **a** MGMT promoter methylated vs. unmethylated tumors. **b** IDH1 mutant vs. wild type tumors. **c** Chromosome 10 monosomy vs. polysomy. **d** PTEN deficiency vs. PTEN intact. **e** EGFR-amplified vs. not amplified tumors. **f** EGFRvIII mutant vs. wild-type tumors

incomplete enhancing tumors, while contrast-enhancing tumors tended to have overexpression of genes associated with the hypoxia–angiogenesis–edema pathway in GBM, notably VEGF [45, 46] as well as matrix metalloproteinase-7 (MMP7), which is thought to be involved in the destruction of the extracellular matrix and tumor cell invasion [47]. Using similar radiographic descriptive features, Diehn et al. [38] confirmed these observations, showing that contrast-enhancing tumors had upregulated activity of the hypoxia module, consisting of VEGF, ADM, PLAUR, SERPINE1, and CA12 [48]. These investigators also noted a strong association between the presence of mass effect and a proliferation gene expression signature involving genes associated with proliferation and cell-cycle progression (TOPA, CDC2, and BUB1B) [49], suggesting that tumors with infiltrative nonenhancing tumor share gene expression programs with glial progenitors or CNS stem cells and genes associated with gliogenesis.

A study by Carrillo et al. [37] utilized the same feature set introduced by Pope et al. [12•] to describe the relationship between radiographic features, IDH1 mutational status, MGMT promoter methylation status, and clinical variables in 202 patients with GBM. Investigators noted that the amount of edema present in MR scans could further stratify survival in patients with MGMT methylated tumors, but this association was not present with unmethylated tumors. Additionally, investigators noted the same associations with IDH1 mutation status and predominance in the frontal lobe, as well as the association between lack of contrast enhancement and IDH1 status.

In an attempt to standardize the methodology relating to radiographic descriptive features for GBM, investigators at The Cancer Imaging Archive (TCIA) created the "VASARI" terminology [50, 51]. Largely drawing from the features presented earlier by Pope et al. [12•], the VASARI feature set consists of 24 radiological elements used to describe the morphology of brain tumors on routine contrast-enhanced T1-weighted images (see https://wiki.cancerimagingarchive.net/display/VASARI+Research+Project). Using the set of VASARI features, Colen et al. [52] found that tumors

containing invasive imaging characteristics including deep white matter tract involvement, enhancement that crossed the midline, and the presence of abnormal MR signal intensity involving the internal capsule or brain stem were shown to be associated with upregulation of the MYC oncogene, which along with p53 are considered significant regulators of metabolism. [53, 54], is thought to facilitate aerobic glycolysis [55], and is involved in the maintenance of stem cell self-renewal ability and tumorigenesis [56, 57].

In summary, scientific evidence appears to support the hypothesis that genetic and/or molecular alterations within GBM manifest as specific, macroscopic, observable changes in standard anatomic imaging. General radiographic features including contrast enhancement on post-contrast T1-weighted images, hypointensity on pre-contrast T1-weighted images, and hyperintensity on T2-weighted images are associated with common histological attributes within the underlying tumor tissues, namely angiogenesis, proliferative tumor, macroscopic necrosis, edema, and nonenhancing tumor. Using these basic features, investigators have shown that tumor location, composition, sizes, and descriptive features can be used to identify more complex biological behaviors relating to genetic and molecular programs activated or inhibited in individual tumors.

Diffusion MRI–Pathology Correlations

Although anatomical imaging appears to capture specific biological characteristics of the underlying tumor tissues, physiologic imaging measures may be able to provide additional insight into the functional behavior of these tissues, which is hypothesized to be reflective of inherent genomic or molecular programs. Diffusion-weighted imaging (DWI) is an MR imaging technique that allows for quantification of microscopic, subvoxel water motion for which an apparent diffusion coefficient (ADC) can be estimated, which reflects the overall magnitude of water motion. Diffusion tensor imaging (DTI) is a DWI technique in which the magnitude and direction of water self-diffusion are quantified. In densely packed tumor regions, investigators have hypothesized that cell membranes and other structures restrict free movement of water molecules, resulting in a lower measured ADC [58]. Subsequent studies have supported this hypothesis, particularly in treatment of naïve tumors, empirically demonstrating a negative correlation with tumor cell density [58–65]. This relationship can be confounded by a number of factors including ischemia [66, 67], differences in cell shape [68, 69], and the presence of infection or inflammation [70–72]. Thus, changes in DWI or DTI parameters are to be interpreted with caution, particularly during therapeutic interventions.

An image-guided biopsy study performed by Barajas et al. [73••] examined the regional variations in histopathological features in anatomical and physiologic MR images. Investigators noted that diffusion MR parameters including relative ADC (i.e., ADC within the tumor relative to normal-appearing contralateral white matter) and relative fractional anisotropy or FA, a scalar measure relating to the directional dependence of water self-diffusion derived from the diffusion tensor [74, 75], within areas of nonenhancing tumor showed a significant association with key histopathologic features. In particular, this study showed that ADC was inversely correlated with "tumor score," a composite parameter with a host of histological features, as well as proliferation rate observed on Ki-67 IHC and architectural disruption noted on SMI-31 staining. Additionally, FA was shown to be positively correlated with delicate microvasculature as well as architectural disruption. Together, these results support the hypothesis that low measures of tumor ADC are associated with more aggressive histological features in GBM.

Instead of using mean values within a tumor region of interest, a study by Pope et al. [76] utilized the distribution of ADC values within pre-treatment contrast-enhancing regions to predict the response to bevacizumab. Specifically, this study fits a double Gaussian mixture model to the ADC histogram extracted from pre-treatment contrast-enhancing regions and noted that the mean of the lower ADC histogram, ADC_L, was a significant predictor of both PFS and OS. Consistent with the hypothesis that lower mean ADC_L may be a worse prognosis due to higher cellularity and higher proliferation rate, this study and a separate independent multicenter study [77] confirmed that lower mean ADC_L values were correlated with shortened survival. Interestingly, another study by Pope et al. [78] also applied this same technique, but to newly diagnosed GBM patients treated with bevacizumab and found opposite trends. Specifically, this study suggested that GBM patients with *higher* ADC_L actually had *lower* PFS compared to that with patients having lower ADC_L; however, this study also demonstrated that patients with a higher ADC_L treated with placebo upfront had a longer post-progression survival when treated with bevacizumab at recurrence, suggesting a higher ADC_L that may be favorable for treatment with bevacizumab at recurrence and not in the upfront setting.

Evidence suggests this effect may be due to the apparent differential response of gene expression subtypes to bevacizumab. A recent study by Phillips et al. [79] demonstrated that GBM with the proneural signature had a significantly longer PFS and OS when treated with bevacizumab upfront compared to that with the other phenotypes. Additionally, this study demonstrated that the mesenchymal phenotype had a significantly longer post-progression survival, particularly in the placebo arm where patients received bevacizumab at recurrence, which suggests this phenotype may have a significant survival advantage when treated with bevacizumab

at recurrence, but not when given upfront with radiation and temozolomide. Also, tumors with the proliferative gene expression signature did poorly in both the upfront and recurrent setting. When examining the pre-surgical, pre-treatment ADC_L characteristics in 31 GBMs with known gene expression phenotypes (Fig. 3), results suggested mesenchymal tumors tended to have a higher ADC_L, proneural tumors tended to have a lower ADC_L, and proliferative tumors were always shown to have a significantly lower ADC_L when compared with the prognostic threshold of 1.2 μm^2/ms. These results imply that mesenchymal tumors, which tend to have an ADC_L >1.2 μm^2/ms, do not have a benefit from bevacizumab upfront but instead show a survival benefit when given at recurrence. Results also imply that proneural tumors, which tend to have an ADC_L <1.2 μm^2/ms, show a survival benefit upfront but not at recurrence. Lastly, proliferative tumors which almost always appear to have an ADC_L <1.2 μm^2/ms tend to do poorly regardless of when bevacizumab therapy is delivered.

In addition to the relationship between gene expression subtypes and diffusion parameters, a separate study by Pope et al. [80•] attempted to explore novel associations between gene expression and ADC histogram parameters independent of predefined subclassifications. Investigators noted that a total of 13 genes were expressed at twofold or greater levels in tumors with high ADC_L compared to that with tumors exhibiting low ADC_L characteristics. Approximately half of these genes were associated with collagen or collagen-binding proteins within the extracellular matrix, including decorin. These results suggest tumors with higher ADC_L may be associated with more of a proinvasive phenotype, which appears consistent with known characteristics of the mesenchymal GBM subtype.

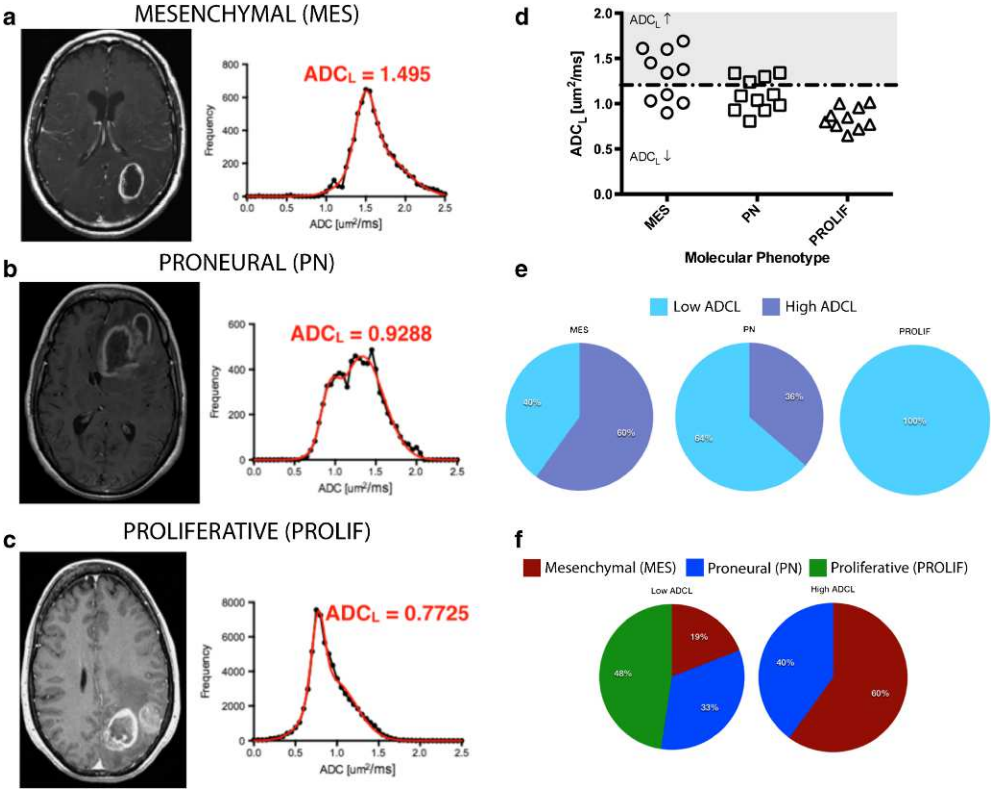

Fig. 3 Diffusion characteristics of gene expression subtypes. **a** Representative post-contrast T1-weighted image and ADC histogram for a patient with a mesenchymal (MES) tumor showing elevated ADC_L. **b** Representative post-contrast T1-weighted image and ADC histogram for a patient with a proneural (PH) tumor showing relatively low ADC_L. **c** Representative post-contrast T1-weighted image and ADC histogram for a patient with a proliferative (PROLIF) tumor subtype showing low ADC_L. **d** Distribution of high and low ADC_L for the various phenotypes. **e** Distribution of high vs. low ADC_L for each individual phenotype. **f** Approximate proportion of phenotypes within each ADC_L classification

In addition to differences in diffusion characteristics in gene expression subtypes, examination of our probabilistic radiographic atlas has suggested that there may be subtle yet significant differences in diffusion characteristics between MGMT promoter methylated and unmethylated GBM. In particular, we examined pre-surgical, pre-treatment ADC maps in 185 GBM tumors (70 MGMT methylated and 115 MGMT unmethylated) and noticed that mean ADC within contrast-enhancing tumor was significantly higher in MGMT unmethylated tumors (Fig. 4a; Methylated group median ADC=1.189 μm^2/ms vs. unmethylated group median ADC=1.288 μm^2/ms; Mann–Whitney test, P=0.030). Additionally, results suggest the absolute value of the mean Laplacian of ADC ($|\nabla^2 ADC|$ or the absolute value of the second order spatial gradient of ADC) within areas of T2/FLAIR hyperintense regions may be higher in MGMT unmethylated tumors, suggesting unmethylated tumors may be more spatially heterogeneous whereas methylated tumors may be smoother in texture (Fig. 4b; Methylated group median $|\nabla^2 ADC|$=3.2 ms^{-1} vs. unmethylated group median $|\nabla^2 ADC|$=4.1 ms^{-1}; Mann–Whitney test, P=0.023). This observation appears consistent with a previous report from Drabycz et al. [81], which demonstrated higher spatial frequencies in MGMT unmethylated tumors using T2-weighted images and further implies that more sophisticated image features like texture may provide additional insight into the underlying biology within spatially heterogeneous tumor tissues.

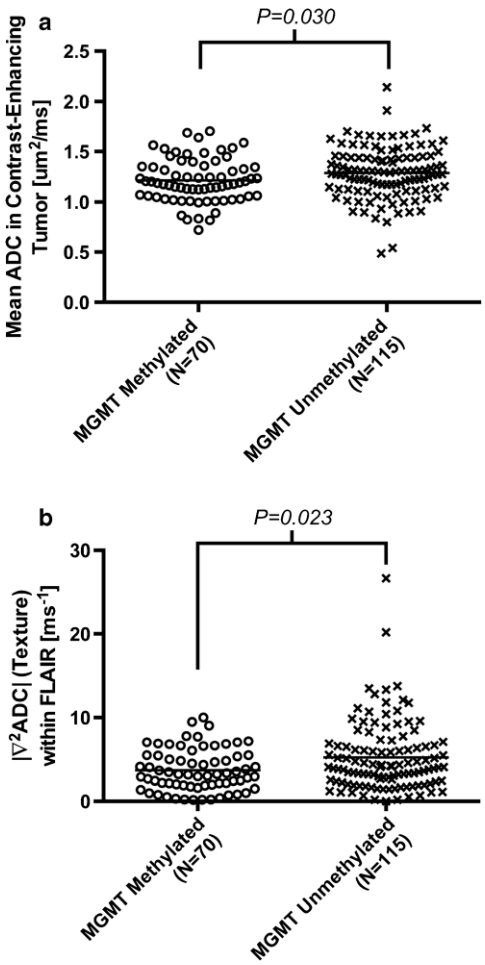

Fig. 4 Diffusion and diffusion texture features for MGMT promoter methylated (N=70) and unmethylated (N=115) tumors. **a** A difference in mean ADC within the contrast-enhancement tumor was observed between MGMT promoter methylated and unmethylated tumors. **b** Additionally, a difference in the absolute value of the Laplacian of ADC, a measure of texture or spatial heterogeneity, was detected between MGMT methylated and unmethylated tumors

Perfusion MRI–Pathology Correlation

Perfusion MRI techniques have been used for nearly 20 years for the evaluation of brain tumors. Dynamic susceptibility contrast (DSC)-MRI, the most commonly used perfusion MR imaging technique for GBM, is a first-pass bolus imaging technique based on the indicator–dilution method [82, 83] and was introduced in the late 1980s [84–90] as a method of estimating relative cerebral blood volume (rCBV), flow (rCBF), and mean transit time (MTT) using the magnetic susceptibility properties of paramagnetic contrast agents (e.g., Gadolinium and other lanthanide chelates) and T2*-weighted MR acquisition methods. Other DSC parameters that have been proposed include relative peak height (rPH), which is related to measures of rCBV given equivalent bolus duration, and percentage of signal intensity recovery (PSR), which is related to capillary permeability. Various investigations have shown that these perfusion parameters reflect important biological information regarding tumor vascular morphometry [73••, 91–93]. In particular, studies have shown that the ratio of relaxation rates R_2* to R_2, corresponding to the change in relaxation rate during a gradient echo vs. a spin echo planar acquisition, respectively, is correlated with mean vessel diameter, since gradient echo acquisition is sensitive to all vessel sizes and spin echo acquisition is sensitive to only microvasculature [94]. Additionally, an early animal study by Cha et al. [91] demonstrated that maximum rCBV was a significant predictor of mean vessel diameter, suggesting DSC-MRI estimates of blood volume may be a valuable surrogate for vessel morphology. Despite these promising results, other investigators have noted that these associations

are highly dependent on acquisition parameters and methods relating to histological evaluation, particularly noting that slice thickness of imaging and histology and fractional vessel area needs to be taken into consideration [92]. Consistent with these previous studies, Barajas et al. [73••] examined DSC-MRI parameters from image-guided biopsy samples and noted that rCBV showed a positive correlation with composite tumor score, proliferation rate, total microvasculature, necrosis, and tumor cell per high-power field. Additionally, this study showed that rPH, which is highly dependent on the specific acquisition parameters, showed similar correlations with composite tumor score, total microvasculature, simple microvasculature score, and tumor cell number per high-power field. Together, these results suggest DSC-MRI measure of rCBV may be a valuable surrogate for characterizing neovasculature in GBM.

Interestingly, tumors with a significant oligodendroglioma component tend to have higher rCBV, independent of high-grade histopathology. Studies by Lev et al. [95] and Cha et al. [96] both confirmed this trend, demonstrating that low-grade oligodendrogliomas often had elevated rCBV compared to that with astrocytomas of similar grade. Additionally, a study by Whitmore et al. [97] examined grades II and III oligodendrogliomas and compared perfusion parameters between groups based on 1p and 19q status, noting that low-grade oligodendrogliomas with loss of heterozygosity in 1p or 1p/19q had a significantly higher rCBV compared to that with low-grade oligodendrogliomas exhibiting either intact alleles or loss of heterozygosity in 19q alone.

Based on these associations and the observation that the proneural signature tends to be enriched in oligodendrogliomas [98], we might hypothesize that proneural tumors may have elevated rCBV compared to other subtypes. In an attempt to test this hypothesis, a recent study by Jain et al. [99] examined DSC-MRI data, TCGA dataset. Investigators noted no significant differences in rCBV measures between gene expression subtypes, either those by Phillips et al. [8•] or Verhaak et al. [4•]. Interestingly, investigators did observe a relatively higher mean and variability when estimating maximum rCBV in proneural tumors. Based on these results, there does not appear to be sufficient evidence to suggest perfusion MRI differs between gene expression subtypes.

Conclusion

In summary, radiogenomics is a provocative new area of research based on decades of previous work examining the association between radiological and histological features. Many generalized associations exist between anatomical imaging and histological features based on this extensive body of knowledge; however, more sophisticated associations between imaging features including tumor location, size, composition, texture, water diffusivity, and perfusion measurements and genomic or molecular programs have only recently been uncovered. Although current results are thought provoking, future studies extending beyond simple radiology–histology associations are warranted in order to establish radiogenomic analyses as tools for prospectively identifying patient subtypes that may benefit from specific therapies.

Compliance with Ethics Guidelines

Conflict of Interest Benjamin M. Ellingson has received the following research support: Roche/Genentech Research Grant, NIH/NCI R21CA167354, UCLA Jonsson Comprehensive Cancer Center Seed Grant, UCLA Radiology Exploratory Research Grant. University of California Cancer Research Coordinating Committee Grant, ACRIN Young Investigator Initiative Grant, National Brain Tumor Society Research Grant, and Siemens Healthcare Research Grant.

Human and Animal Rights and Informed Consent This article does not contain any studies with human or animal subjects performed by the author.

References

Papers of particular interest, published recently, have been highlighted as:
- • Of importance
- •• Of major importance

1. Ostrom QT, Gittleman H, Farah P, Ondracek A, Chen Y, Wolinsky Y, et al. CBTRUS statistical report: primary brain and central nervous system tumors diagnosed in the United States in 2006–2010. Neuro Oncol. 2013;15 Suppl 2: ii1–56.
2. Stupp R, Mason WP, van den Bent MJ, Weller M, Fisher B, Taphoorn MJ, et al. Radiotherapy plus concomitant and adjuvant temozolomide for glioblastoma. N Engl J Med. 2005;352:987–96.
3. Stupp R, Hegi ME, Mason WP, van den Bent MJ, Taphoorn MJ, Janzer RC, et al. Effects of radiotherapy with concomitant and adjuvant temozolomide versus radiotherapy alone on survival in glioblastoma in a randomised phase III study: 5-year analysis of the EORTC-NCIC trial. Lancet Oncol. 2009;10:459–66.
4.• Verhaak RG, Hoadley KA, Purdom E, Wang V, Qi Y, Wilkerson MD, et al. Integrated genomic analysis identifies clinically relevant subtypes of glioblastoma characterized by abnormalities in PDGFRA, IDH1, EGFR, and NF1. Cancer Cell. 2010;17:98–110. *Defines prognostically important gene expression subtypes in GBM.*
5. Rivera AL, Pelloski CE, Gilbert MR, Colman H, De La Cruz C, Sulman EP, et al. MGMT promoter methylation is predictive of response to radiotherapy and prognostic in the absence of adjuvant alkylating chemotherapy for glioblastoma. Neuro Oncol. 2010;12:116–21.
6. Esteller M, Garcia-Foncillas J, Andion E, Goodman SN, Hidalgo OF, Vanaclocha V, et al. Inactivation of the DNA-repair gene MGMT and the clinical response of gliomas to alkylating agents. N Engl J Med. 2000;343:1350–4.
7.• Hegi ME, Diserens AC, Gorlia T, Hamou MF, de Tribolet N, Weller M, et al. MGMT gene silencing and benefit from temozolomide in

glioblastoma. N Engl J Med. 2005;352:997–1003. *Study demonstrates significant therapeutic benefit of temozolomide therapy in MGMT promoter methylated GBM.*

8.• Phillips HS, Kharbanda S, Chen R, Forrest WF, Soriano RH, Wu TD, et al. Molecular subclasses of high-grade glioma predict prognosis, delineate a pattern of disease progression, and resemble stages in neurogenesis. Cancer Cell. 2006;9:157–73. *Defines prognostically important gene expression subtypes of GBM.*

9. Pierallini A, Bonamini M, Pantano P, Palmeggiani F, Raguso M, Osti MF, et al. Radiological assessment of necrosis in glioblastoma: variability and prognostic value. Neuroradiology. 1998;40:150–3.

10. Hammoud MA, Sawaya R, Shi W, Thall PF, Leeds NE. Prognostic significance of preoperative MRI scans in glioblastoma multiforme. J Neurooncol. 1996;27:65–73.

11. Lacroix M, Abi-Said D, Fourney DR, Gokaslan ZL, Shi W, DeMonte F, et al. A multivariate analysis of 416 patients with glioblastoma multiforme: prognosis, extent of resection, and survival. J Neurosurg. 2001;95:190–8.

12.• Pope WB, Sayre J, Perlina A, Villablanca JP, Mischel PS, Cloughesy TF. MR imaging correlates of survival in patients with high-grade gliomas. AJNR Am J Neuroradiol. 2005;26:2466–74. *First study to define radiographic descriptive features for use in radiogenomic analysis. Forms the basis of the VASARI feature set used by TCGA.*

13.•• Ellingson BM, Lai A, Harris RJ, Selfridge JM, Yong WH, Das K, et al. Probabilistic radiographic atlas of glioblastoma phenotypes. AJNR Am J Neuroradiol. 2013;34:533–40. *Study correlates tumor location, volumes, and composition with clinical, molecular, genomic, and interventional phenotypes in >500 GBM patients.*

14. Hobbs SK, Shi G, Homer R, Harsh G, Atlas SW, Bednarski MD. Magnetic resonance image-guided proteomics of human glioblastoma multiforme. J Magn Reson Imaging. 2003;18:530–6.

15.• Rees JH, Smirniotopoulos JG, Jones RV, Wong K. Glioblastoma multiforme: radiologic-pathologic correlation. Radiographics. 1996;16:1413–38. *Quiz 1462–1413. One of the first studies to explicitly define radiographic–pathologic correlations in GBM.*

16. Russell SM, Elliott R, Forshaw D, Golfinos JG, Nelson PK, Kelly PJ. Glioma vascularity correlates with reduced patient survival and increased malignancy. Surg Neurol. 2009;72:242–6. *Discussion 246–247.*

17. Loges S, Mazzone M, Hohensinner P, Carmeliet P. Silencing or fueling metastasis with VEGF inhibitors: antiangiogenesis revisited. Cancer Cell. 2009;15:167–70.

18. Kelly PJ, Daumas-Duport C, Kispert DB, Kall BA, Scheithauer BW, Illig JJ. Imaging-based stereotaxic serial biopsies in untreated intracranial glial neoplasms. J Neurosurg. 1987;66:865–74.

19. Folkman J. Role of angiogenesis in tumor growth and metastasis. Semin Oncol. 2002;29:15–8.

20.•• Pope WB, Chen JH, Dong J, Carlson MR, Perlina A, Cloughesy TF, et al. Relationship between gene expression and enhancement in glioblastoma multiforme: exploratory DNA microarray analysis. Radiology. 2008;249:268–77. *One of the first radiogenomic studies in GBM.*

21. Damadian R. Tumor detection by nuclear magnetic resonance. Science. 1971;171:1151–3.

22. Hoehn-Berlage M, Tolxdorff T, Bockhorst K, Okada Y, Ernestus RI. In vivo NMR T2 relaxation of experimental brain tumors in the cat: a multiparameter tissue characterization. Magn Reson Imaging. 1992;10:935–47.

23. Oh J, Cha S, Aiken AH, Han ET, Crane JC, Stainsby JA, et al. Quantitative apparent diffusion coefficients and T2 relaxation times in characterizing contrast enhancing brain tumors and regions of peritumoral edema. J Magn Reson Imaging. 2005;21:701–8.

24. Levin VA, Crafts DC, Norman DM, Hoffer PB, Spire JP, Wilson CB. Criteria for evaluating patients undergoing chemotherapy for malignant brain tumors. J Neurosurg. 1977;47:329–35.

25. Miller AB, Hoogstraten B, Staquet M, Winkler A. Reporting results of cancer treatment. Cancer. 1981;47:207–14.

26. Macdonald DR, Cascino TL, Schold Jr SC, Cairncross JG. Response criteria for phase II studies of supratentorial malignant glioma. J Clin Oncol. 1990;8:1277–80.

27. Wen PY, Macdonald DR, Reardon DA, Cloughesy TF, Sorensen AG, Galanis E, et al. Updated response assessment criteria for high-grade gliomas: response assessment in neuro-oncology working group. J Clin Oncol. 2010;28:1963–72.

28. Simpson JR, Horton J, Scott C, Curran WJ, Rubin P, Fischbach J, et al. Influence of location and extent of surgical resection on survival of patients with glioblastoma multiforme: results of three consecutive Radiation Therapy Oncology Group (RTOG) clinical trials. Int J Radiat Oncol Biol Phys. 1993;26:239–44.

29. Sanai N, Alvarez-Buylla A, Berger MS. Neural stem cells and the origin of gliomas. N Engl J Med. 2005;353:811–22.

30. Wechsler-Reya R, Scott MP. The developmental biology of brain tumors. Annu Rev Neurosci. 2001;24:385–428.

31. Zlatescu MC, TehraniYazdi A, Sasaki H, Megyesi JF, Betensky RA, Louis DN, et al. Tumor location and growth pattern correlate with genetic signature in oligodendroglial neoplasms. Cancer Res. 2001;61:6713–5.

32. Marino S, Vooijs M, van Der Gulden H, Jonkers J, Berns A. Induction of medulloblastomas in p53-null mutant mice by somatic inactivation of Rb in the external granular layer cells of the cerebellum. Genes Dev. 2000;14:994–1004.

33. Poppleton H, Gilbertson RJ. Stem cells of ependymoma. Br J Cancer. 2007;96:6–10.

34. Lai A, Kharbanda S, Pope WB, Tran A, Solis OE, Peale F, et al. Evidence for sequenced molecular evolution of IDH1 mutant glioblastoma from a distinct cell of origin. J Clin Oncol. 2011;29:4482–90.

35. Ellingson BM, Cloughesy TF, Pope WB, Zaw TM, Phillips H, Lalezari S, et al. Anatomic localization of O6-methylguanine DNA methyltransferase (MGMT) promoter methylated and unmethylated tumors: a radiographic study in 358 de novo human glioblastomas. Neuroimage. 2012;59:908–16.

36. Lim DA, Cha S, Mayo MC, Chen MH, Keles E, VandenBerg S, et al. Relationship of glioblastoma multiforme to neural stem cell regions predicts invasive and multifocal tumor phenotype. Neuro Oncol. 2007;9:424–9.

37. Carrillo JA, Lai A, Nghiemphu PL, Kim HJ, Phillips HS, Kharbanda S, et al. Relationship between tumor enhancement, edema, IDH1 mutational status, MGMT promoter methylation, and survival in glioblastoma. AJNR Am J Neuroradiol. 2012;33:1349–55.

38. Diehn M, Nardini C, Wang DS, McGovern S, Jayaraman M, Liang Y, et al. Identification of noninvasive imaging surrogates for brain tumor gene-expression modules. Proc Natl Acad Sci U S A. 2008;105:5213–8.

39.• Nacini KM, Pope WB, Cloughesy TF, Harris RJ, Lai A, Eskin A, et al. Identifying the mesenchymal molecular subtype of glioblastoma using quantitative volumetric analysis of anatomic magnetic resonance images. Neuro Oncol. 2013;15:626–34. *Study demonstrates how simple volumes and tumor composition can be used to identify the mesenchymal gene expression subtype of GBM.*

40.• Zinn PO, Mahajan B, Sathyan P, Singh SK, Majumder S, Jolesz FA, et al. Radiogenomic mapping of edema/cellular invasion MRI-phenotypes in glioblastoma multiforme. PLoS One. 2011;6:e25451. *One of the first studies to identify novel genomic signatures solely on the basis of predefined radiographic phenotypes.*

41. Zinn PO, Sathyan P, Mahajan B, Bruyere J, Hegi M, Majumder S, et al. A novel volume-age-KPS (VAK) glioblastoma classification identifies a prognostic cognate microRNA-gene signature. PLoS One. 2012;7:e41522.

42. Gutman DA, Cooper LA, Hwang SN, Holder CA, Gao J, Aurora TD, et al. MR imaging predictors of molecular profile and survival: multi-institutional study of the TCGA glioblastoma data set. Radiology. 2013;267:560–9.
43. Kuo MD, Gollub J, Sirlin CB, Ooi C, Chen X. Radiogenomic analysis to identify imaging phenotypes associated with drug response gene expression programs in hepatocellular carcinoma. J Vasc Interv Radiol. 2007;18:821–31.
44. Rutman AM, Kuo MD. Radiogenomics: creating a link between molecular diagnostics and diagnostic imaging. Eur J Radiol. 2009;70:232–41.
45. Fischer I, Gagner JP, Law M, Newcomb EW, Zagzag D. Angiogenesis in gliomas: biology and molecular pathophysiology. Brain Pathol. 2005;15:297–310.
46. Jain RK, di Tomaso E, Duda DG, Loeffler JS, Sorensen AG, Batchelor TT. Angiogenesis in brain tumours. Nat Rev Neurosci. 2007;8:610–22.
47. Rome C, Arsaut J, Taris C, Couillaud F, Loiseau H. MMP-7 (matrilysin) expression in human brain tumors. Mol Carcinog. 2007;46:446–52.
48. Leo C, Giaccia AJ, Denko NC. The hypoxic tumor microenvironment and gene expression. Semin Radiat Oncol. 2004;14:207–14.
49. Whitfield ML, Sherlock G, Saldanha AJ, Murray JI, Ball CA, Alexander KE, et al. Identification of genes periodically expressed in the human cell cycle and their expression in tumors. Mol Biol Cell. 2002;13:1977–2000.
50. Channin DS, Mongkolwat P, Kleper V, Rubin DL. The annotation and image mark-up project. Radiology. 2009;253:590–2.
51. Channin DS, Mongkolwat P, Kleper V, Sepukar K, Rubin DL. The caBIG annotation and image Markup project. J Digit Imaging. 2010;23:217–25.
52. Colen RR, Vangel M, Wang J, Gutman DA, Hwang SN, Wintermark M, et al. Imaging genomic mapping of an invasive MRI phenotype predicts patient outcome and metabolic dysfunction: a TCGA glioma phenotype research group project. BMC Med Genomics. 2014;7:30.
53. Vander Heiden MG, Cantley LC, Thompson CB. Understanding the Warburg effect: the metabolic requirements of cell proliferation. Science. 2009;324:1029–33.
54. Dang CV. MYC, metabolism, cell growth, and tumorigenesis. Cold Spring Harb Perspect Med. 2013;3.
55. Kaadige MR, Elgort MG, Ayer DE. Coordination of glucose and glutamine utilization by an expanded Myc network. Transcription. 2010;1:36–40.
56. Nakagawa M, Koyanagi M, Tanabe K, Takahashi K, Ichisaka T, Aoi T, et al. Generation of induced pluripotent stem cells without Myc from mouse and human fibroblasts. Nat Biotechnol. 2008;26:101–6.
57. Dang CV. MYC on the path to cancer. Cell. 2012;149:22–35.
58. Chenevert TL, Stegman LD, Taylor JM, Robertson PL, Greenberg HS, Rehemtulla A, et al. Diffusion magnetic resonance imaging: an early surrogate marker of therapeutic efficacy in brain tumors. J Natl Cancer Inst. 2000;92:2029–36.
59. Bode MK, Ruohonen J, Nieminen MT, Pyhtinen J. Potential of diffusion imaging in brain tumors: a review. Acta Radiol. 2006;47:585–94.
60. Ellingson BM, Malkin MG, Rand SD, Connelly JM, Quinsey C, LaViolette PS, et al. Validation of functional diffusion maps (fDMs) as a biomarker for human glioma cellularity. J Magn Reson Imaging. 2010;31:538–48.
61. Sugahara T, Korogi Y, Kochi M, Ikushima I, Shigematu Y, Hirai T, et al. Usefulness of diffusion-weighted MRI with echo-planar technique in the evaluation of cellularity in gliomas. J Magn Reson Imaging. 1999;9:53–60.
62. Lyng H, Haraldseth O, Rofstad EK. Measurement of cell density and necrotic fraction in human melanoma xenografts by diffusion weighted magnetic resonance imaging. Magn Reson Med. 2000;43:828–36.
63. Guo AC, Cummings TJ, Dash RC, Provenzale JM. Lymphomas and high-grade astrocytomas: comparison of water diffusibility and histologic characteristics. Radiology. 2002;224:177–83.
64. Hayashida Y, Hirai T, Morishita S, Kitajima M, Murakami R, Korogi Y, et al. Diffusion-weighted imaging of metastatic brain tumors: comparison with histologic type and tumor cellularity. AJNR Am J Neuroradiol. 2006;27:1419–25.
65. Kinoshita M, Hashimoto N, Goto T, Kagawa N, Kishima H, Izumoto S, et al. Fractional anisotropy and tumor cell density of the tumor core show positive correlation in diffusion tensor magnetic resonance imaging of malignant brain tumors. Neuroimage. 2008;43:29–35.
66. Kidwell CS, Alger JR, Di Salle F, Starkman S, Villablanca P, Bentson J, et al. Diffusion MRI in patients with transient ischemic attacks. Stroke. 1999;30:1174–80.
67. Pierpaoli C, Alger JR, Righini A, Mattiello J, Dickerson R, Des Pres D, et al. High temporal resolution diffusion MRI of global cerebral ischemia and reperfusion. J Cereb Blood Flow Metab. 1996;16:892–905.
68. Verheul HB, Balazs R, van der Sprenkel JW B, Tulleken CA, Nicolay K, Tamminga KS, et al. Comparison of diffusion-weighted MRI with changes in cell volume in a rat model of brain injury. NMR Biomed. 1994;7:96–100.
69. Wintersperger BJ, Runge VM, Biswas J, Reiser MF, Schoenberg SO. Brain tumor enhancement in MR imaging at 3 Tesla: comparison of SNR and CNR gain using TSE and GRE techniques. Invest Radiol. 2007;42:558–63.
70. Chang SC, Lai PH, Chen WL, Weng HH, Ho JT, Wang JS, et al. Diffusion-weighted MRI features of brain abscess and cystic or necrotic brain tumors: comparison with conventional MRI. Clin Imaging. 2002;26:227–36.
71. Farrell CJ, Hoh BL, Pisculli ML, Henson JW, FG 2nd B, Curry Jr WT. Limitations of diffusion-weighted imaging in the diagnosis of postoperative infections. Neurosurgery. 2008;62:577–83. *Discussion 577–583.*
72. Kastrup O, Wanke I, Maschke M. Neuroimaging of infections. NeuroRx. 2005;2:324–32.
73.•• Barajas Jr RF, Phillips JJ, Parvataneni R, Molinaro A, Essock-Burns E, Bourne G, et al. Regional variation in histopathologic features of tumor specimens from treatment-naive glioblastoma correlates with anatomic and physiologic MR Imaging. Neuro Oncol. 2012;14:942–54. *One of the first studies to use image-guided biopsies to examine the association between physiologic imaging features and histopathology.*
74. Basser PJ, Pierpaoli C. Microstructural and physiological features of tissues elucidated by quantitative-diffusion-tensor MRI. J Magn Reson B. 1996;111:209–19.
75. Basser PJ. New histological and physiological stains derived from diffusion-tensor MR images. Ann N Y Acad Sci. 1997;820:123–38.
76. Pope WB, Kim HJ, Huo J, Alger J, Brown MS, Gjertson D, et al. Recurrent glioblastoma multiforme: ADC histogram analysis predicts response to bevacizumab treatment. Radiology. 2009;252:182–9.
77. Pope WB, Qiao XJ, Kim HJ, Lai A, Nghiemphu P, Xue X, et al. Apparent diffusion coefficient histogram analysis stratifies progression-free and overall survival in patients with recurrent GBM treated with bevacizumab: a multi-center study. J Neurooncol. 2012;108:491–8.
78. Pope WB, Lai A, Mehta R, Kim HJ, Qiao J, Young JR, et al. Apparent diffusion coefficient histogram analysis stratifies progression-free survival in newly diagnosed bevacizumab-treated glioblastoma. AJNR Am J Neuroradiol. 2011;32:882–9.
79. Phillips H, Sandmann T, Li C, Cloughesy TF, Chinot OL, Wick W, et al. Correlation of molecular subtypes with survival in AVAglio

(bevacizumab and radiotherapy and temozolomide for newly diagnosed glioblastoma). J Clin Oncol 2014;32: suppl; abstr 2001.

80.• Pope WB, Mirsadraei L, Lai A, Eskin A, Qiao J, Kim HJ, et al. Differential gene expression in glioblastoma defined by ADC histogram analysis: relationship to extracellular matrix molecules and survival. AJNR Am J Neuroradiol. 2012;33:1059–64. *One of the first studies to explore differences in gene expression on the basis of diffusion MR phenotypes.*

81. Drabycz S, Roldan G, de Robles P, Adler D, McIntyre JB, Magliocco AM, et al. An analysis of image texture, tumor location, and MGMT promoter methylation in glioblastoma using magnetic resonance imaging. Neuroimage. 2010;49:1398–405.

82. Meier P, Zierler KL. On the theory of the indicator-dilution method for measurement of blood flow and volume. J Appl Physiol. 1954;6:731–44.

83. Stewart GN. Researches on the circulation time and on the influences which affect it. J Physiol. 1897;22:159–83.

84. Rosen BR, Belliveau JW, Vevea JM, Brady TJ. Perfusion imaging with NMR contrast agents. Magn Reson Med. 1990;14:249–65.

85. Villringer A, Rosen BR, Belliveau JW, Ackerman JL, Lauffer RB, Buxton RB, et al. Dynamic imaging with lanthanide chelates in normal brain: contrast due to magnetic susceptibility effects. Magn Reson Med. 1988;6:164–74.

86. Rosen BR, Belliveau JW, Buchbinder BR, McKinstry RC, Porkka LM, Kennedy DN, et al. Contrast agents and cerebral hemodynamics. Magn Reson Med. 1991;19:285–92.

87. Belliveau JW, Kennedy Jr DN, McKinstry RC, Buchbinder BR, Weisskoff RM, Cohen MS, et al. Functional mapping of the human visual cortex by magnetic resonance imaging. Science. 1991;254:716–9.

88. Kwong KK, Belliveau JW, Chesler DA, Goldberg IE, Weisskoff RM, Poncelet BP, et al. Dynamic magnetic resonance imaging of human brain activity during primary sensory stimulation. Proc Natl Acad Sci U S A. 1992;89:5675–9.

89. Edelman RR, Mattle HP, Atkinson DJ, Hill T, Finn JP, Mayman C, et al. Cerebral blood flow: assessment with dynamic contrast-enhanced T2*-weighted MR imaging at 1.5 T. Radiology. 1990;176:211–20.

90. Hacklander T, Reichenbach JR, Hofer M, Modder U. Measurement of cerebral blood volume via the relaxing effect of low-dose gadopentetate dimeglumine during bolus transit. AJNR Am J Neuroradiol. 1996;17:821–30.

91. Cha S, Johnson G, Wadghiri YZ, Jin O, Babb J, Zagzag D, et al. Dynamic, contrast-enhanced perfusion MRI in mouse gliomas: correlation with histopathology. Magn Reson Med. 2003;49:848–55.

92. Pathak AP, Schmainda KM, Ward BD, Linderman JR, Rebro KJ, Greene AS. MR-derived cerebral blood volume maps: issues regarding histological validation and assessment of tumor angiogenesis. Magn Reson Med. 2001;46:735–47.

93. Badruddoja MA, Krouwer HG, Rand SD, Rebro KJ, Pathak AP, Schmainda KM. Antiangiogenic effects of dexamethasone in 9L gliosarcoma assessed by MRI cerebral blood volume maps. Neuro Oncol. 2003;5:235–43.

94. Dennie J, Mandeville JB, Boxerman JL, Packard SD, Rosen BR, Weisskoff RM. NMR imaging of changes in vascular morphology due to tumor angiogenesis. Magn Reson Med. 1998;40:793–9.

95. Lev MH, Ozsunar Y, Henson JW, Rasheed AA, Barest GD, Harsh GR, et al. Glial tumor grading and outcome prediction using dynamic spin-echo MR susceptibility mapping compared with conventional contrast-enhanced MR: confounding effect of elevated rCBV of oligodendrogliomas [corrected]. AJNR Am J Neuroradiol. 2004;25:214–21.

96. Cha S, Tihan T, Crawford F, Fischbein NJ, Chang S, Bollen A, et al. Differentiation of low-grade oligodendrogliomas from low-grade astrocytomas by using quantitative blood-volume measurements derived from dynamic susceptibility contrast-enhanced MR imaging. AJNR Am J Neuroradiol. 2005;26:266–73.

97. Whitmore RG, Krejza J, Kapoor GS, Huse J, Woo JH, Bloom S, et al. Prediction of oligodendroglial tumor subtype and grade using perfusion weighted magnetic resonance imaging. J Neurosurg. 2007;107:600–9.

98. Cooper LA, Gutman DA, Long Q, Johnson BA, Cholleti SR, Kurc T, et al. The proneural molecular signature is enriched in oligodendrogliomas and predicts improved survival among diffuse gliomas. PLoS One. 2010;5:e12548.

99. Jain R, Poisson L, Narang J, Gutman D, Scarpace L, Hwang SN, et al. Genomic mapping and survival prediction in glioblastoma: molecular subclassification strengthened by hemodynamic imaging biomarkers. Radiology. 2013;267:212–20.